# Development of Carbon Dioxide Microbubble Sequestration into Saline Aquifer and $CO_2$-EOR Reservoirs

## Introduction

To study the effect of microbubble injection for $CO_2$ dissolution, we carried out laboratory experiments of $CO_2$ flooding in porous sandstone (Berea sandstone). Using X-ray CT image analysis, porosity estimation and $CO_2$ saturation monitoring were conducted. A long core specimen was used to determine how much the microbubble effect reached in our experiment system. On the basis of experimental results, we try to evaluate the superiority of microbubble injection for $CO_2$ dissolution by comparing the difference between microbubble and normal-bubble injections. We expect that the microbubble $CO_2$ injection technique will contribute to geological $CO_2$ sequestration.

## Rock specimen

Berea sandstone (diameter: 34.85mm, length: 288.00mm) was used in this study. It has bedding planes parallel to the core axis. We set the bedding planes horizontally. Microbubble filter (diameter: 34.80mm, length: 4.00mm) was located in between distributer and core specimen in upstream side.

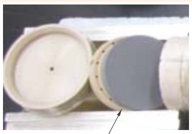

*microbubble filter*

*288mm long core specimen*

*Physical properties of specimen & MB filter*

| | diameter (mm) | length (mm) | bulk volume ($cm^3$) | porosity (%) | sample pore volume ($cm^3$) | permeability (mD) |
|---|---|---|---|---|---|---|
| Berea sandstone | 34.85 | 288.00 | 274.72 | 19.70 | 54.12 | 131 |
| microbubble filter | 34.80 | 4.00 | 3.80 | 31.28 | 1.19 | - |

## Test system

The experiments were carried out under the pressure and temperature conditions that simulate underground environments; pore pressure: 10MPa, temperature: 40 degrees Celsius. The confining pressure of 15MPa was selected in this study. The syringe pumps on the upstream side was controlled to maintain 0.05ml/min (constant flow control). And the syringe pump on the downstream side was controlled to maintain 10 MPa.

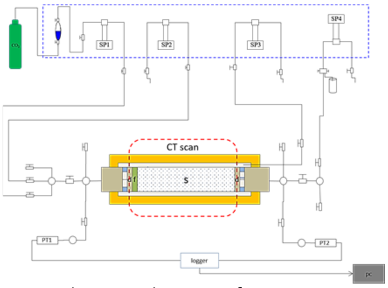


*Schematic diagram of test system*

SP: syringe pump (SP1: $CO_2$, SP2: water, SP3: confining oil, SP4: back pressure), S: rock sample, PT: pressure transducer, d: distributor, f: microbubble filter

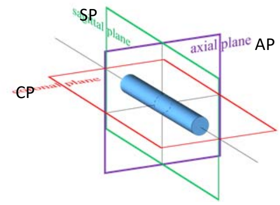


*Major cross Sections in CT*

## microbubble

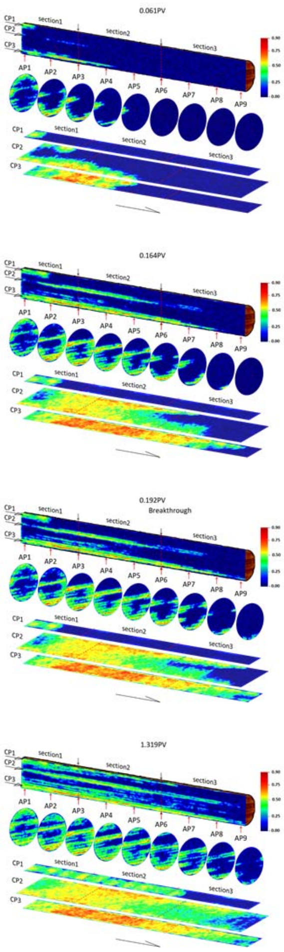


## normal-bubble

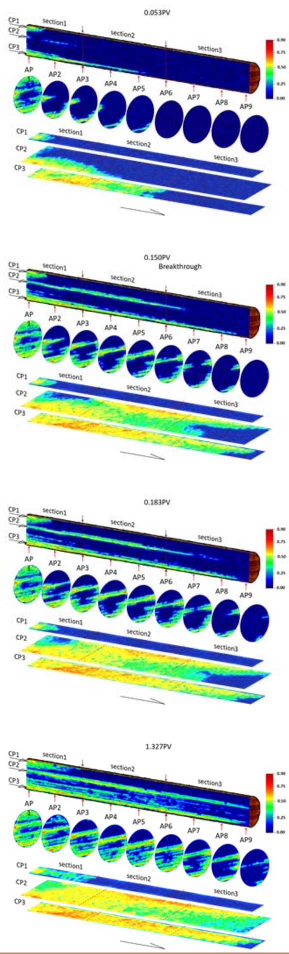


## $CO_2$ saturations

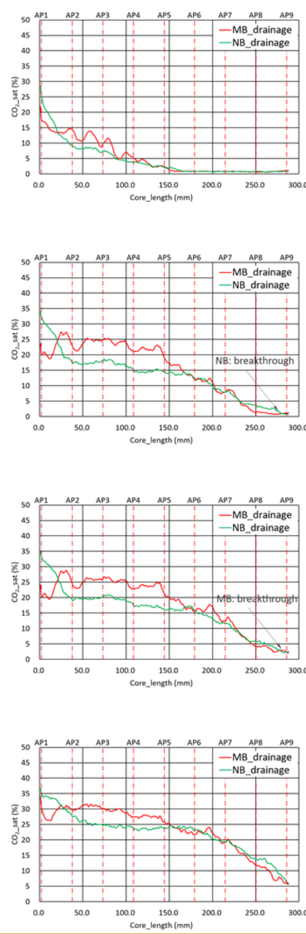


## Field application

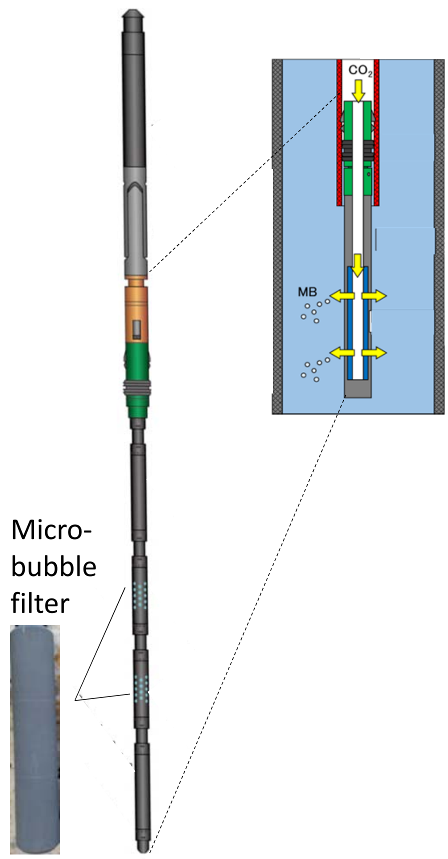


## Conclusions

- $CO_2$-flooding laboratory experiments of porous sandstone (Berea sandstone; long core specimen; 288mm) and X-ray CT visualization were carried out to study the effect of microbubble injection for $CO_2$ dissolution.
- We could estimate the porosity of specimen and visualize the process of water injection and $CO_2$-flooding process by the X-ray CT image analysis. $CO_2$ saturations during the experiments were also obtained.
- The $CO_2$ saturation distributions along the specimen were different in between the cases of microbubble and normal-bubble $CO_2$ injections. At each breakthrough point, there was a difference of about 5% points of $CO_2$ saturation. It reveals that the microbubble $CO_2$ injection has more advantage to the $CO_2$ dissolution for geological $CO_2$ sequestration.

**Acknowledgement :**
This work is part of an R&D project, "Research and Development of Safety Technology for Geological $CO_2$ Storage" by the *Ministry of Economy, Trade and Industry (METI) of Japan*.

RITE
Research Institute of Innovative Technology for the Earth

# 海水中のCO₂濃度（pCO₂）と溶存酸素（DO）の関係を用いた異常値判定基準について

## －大阪湾の長期観測データの解析事例－

**目的**　観測された$pCO_2$から異常値を検出するための次の2つの基準値についてその有効性について検討を行う。
① $pCO_2$一定基準値：季節ごとに設定した一定の$pCO_2$値が閾値　② $pCO_2$-DO基準値：$pCO_2$とDO（溶存酸素）の関係を用いた閾値（Uchimoto et al., 2017）

**解析データ**

**海域**：大阪湾。20測点（図1）のうち測点2-8を鉛直混合の強い西部、測点1, 9-20を成層の強い東部として解析（cf. エスチュアリ循環：城, 1989; 中嶋・藤原, 2007; 図2）

**データ**：浅海定線調査データ（2002年～2010年の2月、5月、8月、11月に底層で観測された水温、塩分、DO、pH; http://kouwan.pa.kkr.mlit.go.jp/kankyo-db）

**$pCO_2$**：塩分から求めた全アルカリ度（田口ら, 2009）とpHを使ってCO2SYSで計算

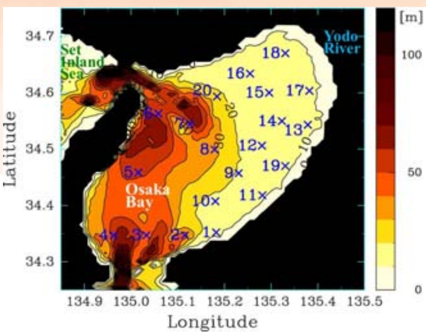

図1: 測点位置と水深（カラー）

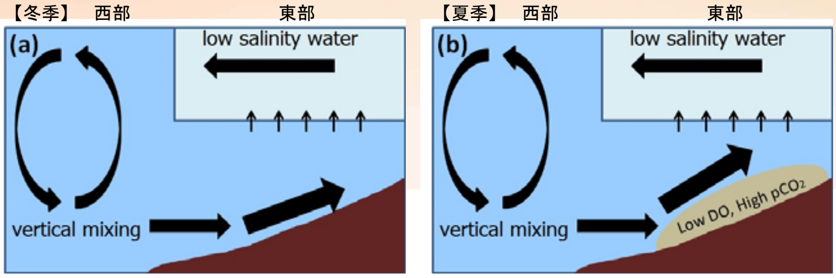

図2: 大阪湾のエスチュアリ循環概念図。(a) 冬季は西部で混合された水が海底に沿って東部に流れ込むため東部底層も高DO, 低$pCO_2$。(b) 夏季は東部の底層より上に流れ込むため東部底層が低DO, 高$pCO_2$になりやすい。（中嶋・藤原, 2007）

**基準値**　①$pCO_2$一定基準値：各月ごとに基準値を決定する。ここでは例として平均値＋2.57σを基準値とした（表1）
②$pCO_2$-DO基準値：$pCO_2$とDO（%）の線形回帰の予測範囲上限を基準値とする。ここでは例として回帰直線の99%予測範囲上限を基準値とした（図3）

| | 2月 | 5月 | 8月 | 11月 |
|---|---|---|---|---|
| 東部 | 455.7 | 811.9 | 1496.2 | 619.7 |
| 西部 | 453.7 | 541.3 | 707.4 | 601.7 |

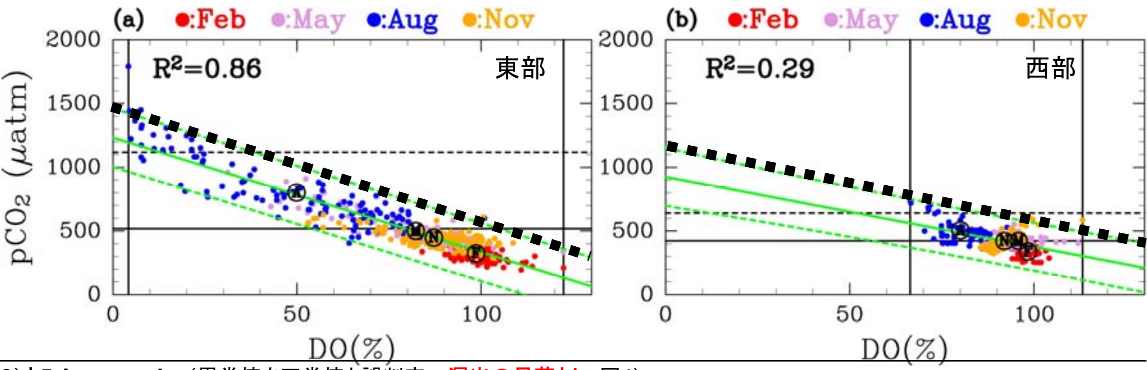

図3（→）: 黒太点線が$pCO_2$-DO基準値（回帰直線（緑実線）の99%予測範囲の上限）。(a) 東部、(b) 西部。黒細実線（横線）は$pCO_2$全データの平均値、黒細点線は$pCO_2$平均値＋2.57σ。黒縦実線はDOの最小値と最大値。

**False-positive**（正常値を異常値と誤判定；表2, 3）と**False-negative**（異常値を正常値と誤判定＝**漏出の見落とし**；図4）

**False-positive**：通年で考えると2つの基準値に大きな違いはないが、$pCO_2$-DO基準値は特定の月にFalse-positiveが集中（東部：8月、西部：11月）

**False-negative**：海域・月によってどちらの基準がよいか（False-negativeが少ないか）は異なる。しかし**$pCO_2$-DO基準値は$\Delta pCO_2$が350μatmで**あれば海域・季節によらずほぼ**漏出の見落としが起きない**（東部の8月でも15%以下）のに対し、**$pCO_2$一定基準値**は東部の夏季に**見落としが約50%以上**になる。

表2: 東部の2002年～2010年のデータに対するFalse-positiveの数。

| 基準値 | 2月 | 5月 | 8月 | 11月 | 計 |
|---|---|---|---|---|---|
| $pCO_2$一定 | 0 (0%) | 3 (2.59%) | 1 (0.86%) | 1 (0.85%) | **5 (1.08%)** |
| $pCO_2$-DO | 0 (0%) | 0 (0%) | 6 (5.17%) | 2 (1.71%) | **8 (1.72%)** |

表3: 西部の2002年～2010年のデータに対するFalse-positiveの数。

| 基準値 | 2月 | 5月 | 8月 | 11月 | 計 |
|---|---|---|---|---|---|
| $pCO_2$一定 | 0 (0%) | 1 (1.59%) | 2 (3.17%) | 1 (1.59%) | **4 (1.59%)** |
| $pCO_2$-DO | 0 (0%) | 0 (0%) | 0 (0%) | 3 (4.76%) | **3 (1.19%)** |

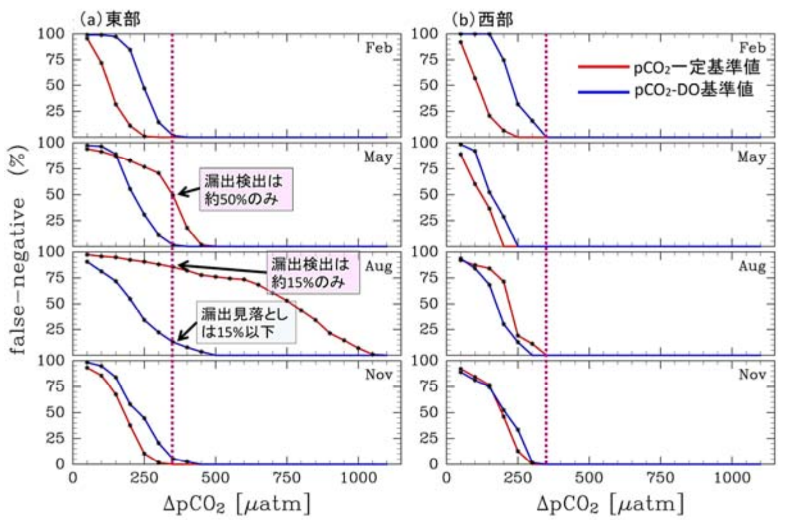

図4（→）: $\Delta pCO_2$（$CO_2$漏出による$pCO_2$の増加）に対するfalse-negativeの割合（%）。赤が$pCO_2$一定基準値、青が$pCO_2$-DO基準値。(a) 東部、(b) 西部。
False-negativeが100%（0%）であれば漏出検出が0%（100%）という意味。

**結論**　$pCO_2$一定基準値と$pCO_2$-DO基準値のどちらがよいかは海域や季節に依存する。$pCO_2$の変動が海面ガス交換の影響を強く受ける海域や季節は$pCO_2$一定基準値の方がよく、海面ガス交換の影響を受けにくい海域や季節では$pCO_2$-DO基準値の方がよい。成層の強い大阪湾東部海域では、底層に海面ガス交換の影響を受けた西部の海水が供給される冬季は$pCO_2$一定基準値の方がよく、底層に西部からの海水が供給されにくい夏季は$pCO_2$一定基準値では漏出検出が極めて困難であり、$pCO_2$-DO基準値が必須となる。一方、年間を通して海面ガス交換の影響の強い西部では、$pCO_2$一定基準値の方が$pCO_2$-DO基準値よりも優れているかまたは同等であり、$pCO_2$の正常異常の判定のためにDOを導入する必要がないと考えられる。

**参考文献**　Uchimoto et al. (2017) Energy Procedia, 114, pp.3771-3777.　城 (1989) 沿岸海洋研究ノート, 26(2), pp.87-98.　田口ら (2009) 沿岸海洋研究, 47(1), pp.71-75.　中嶋・藤原 (2007) 沿岸海洋研究, 44(2), pp.157-163.

**謝辞**　本研究は、経済産業省の「安全なCCS実施のための$CO_2$貯留技術の研究開発事業」の成果の一部である。

RITE
Research Institute of Innovative Technology for the Earth

# Dynamic Stability Monitoring of Geological Formations using Fiber-Optic Sensing

It is important to monitor deformations of geological formations as well as temperature and pressure for a safety evaluation at the CCS site. We are developing a technology to monitor the deformations of the formations using a distributed fiber-optic sensing. Our goal is to deploy fiber-optic cables behind the casing into a deep borehole and cement in place, and the formation deformations (strain) from the surface to the bottom hole are to be monitored continuously in the depth direction.

## 1. Motivation

- At the In Salah field, surface uplift around $CO_2$ injection wells were mapped by InSAR.
- Reservoir expansion induced by pore pressure build-up would go up to the surface.
- If the expansion gets larger safety of a seal layer may be decreased.
- It is important to monitor the deformations from the reservoir to the surface.
- Since measure points are limited for conventional tools, research and development of distributed (multi-point measurable) sensors are required.3

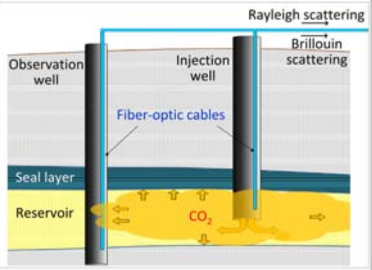


fig. 1 Geological formations monitoring using the optical fibers at the CCS site

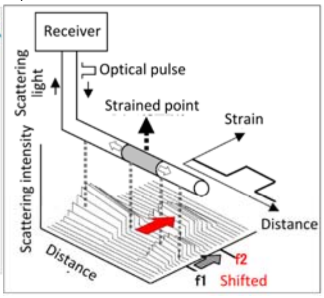


fig. 2 Brillouin gain spectrum measurement

## 2. Measuring method

- When pulsed light is entered into an optic fiber, back scattering lights are induced throughout fiber's length. They produce frequency shifts in proportion to each variation of physical quantity (temperature, pressure and strain).
- These frequency shifts consists of temperature, pressure and strain changes, It is necessary to separate each parameter in case of borehole monitoring (fig. 3).
- Hybrid Brillouin-Rayleigh measurement enables to distinguish among them.

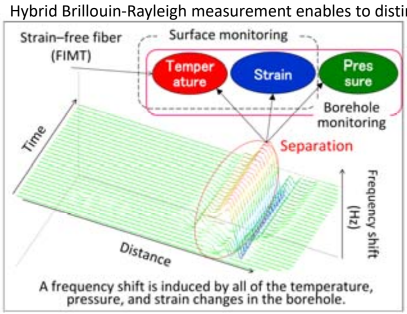


fig. 3 Physical quantities in the frequency shift

✓ Brillouin ($\nu_B$) and Rayleigh ($\nu_R$) scatterings are measured using two fibers which are different in the sensitivity.

✓ There are four formulas for three parameters, temperature, pressure and strain can be separated by:

$$\Delta\nu_B^1 = C_{11}^1\Delta\varepsilon + C_{12}^1\Delta T + C_{13}^1\Delta P$$
$$\Delta\nu_R^1 = C_{21}^1\Delta\varepsilon + C_{22}^1\Delta T + C_{23}^1\Delta P$$
$$\Delta\nu_B^2 = C_{11}^2\Delta\varepsilon + C_{12}^2\Delta T + C_{13}^2\Delta P$$
$$\Delta\nu_R^2 = C_{21}^2\Delta\varepsilon + C_{22}^2\Delta T + C_{23}^2\Delta P$$

fig. 4 Separation of temperature,

## 3. Pilot test -300 m deep borehole-

- The fiber-optic cables were deployed behind the casing (annulus) and cemented in place.

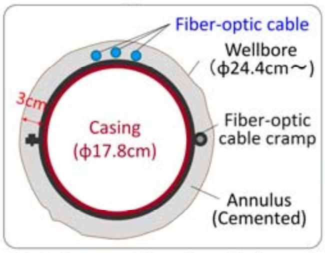


fig. 5 Cross-section of monitoring well

Fiber optic cable clamp

Coupling protector

- A little amount of $CO_2$ was injected into a sand layer through perforation zones of a monitoring well during a day.
- The fibers cemented behind the casing has been successfully applied to measure deformations occurred by $CO_2$ injection at the injection zone.

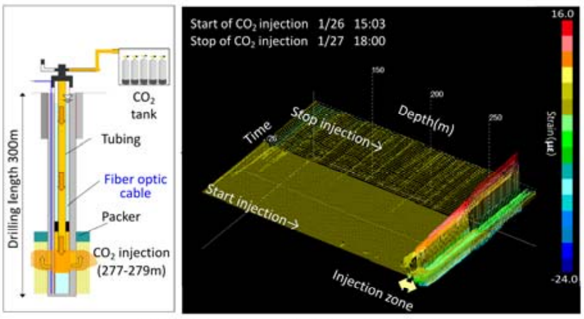


fig. 6 Strains estimated during $CO_2$ injection

## 4. Water pumping test

- Pumping test was performed using two wells, 280 m and 175m away from the monitoring well.
- The pumping zones are sand rich sand-silt alternate layer (aquifer) of 150 m-230 m depth.
- The fibers detected the compression of the aquifer linked with pumping works.

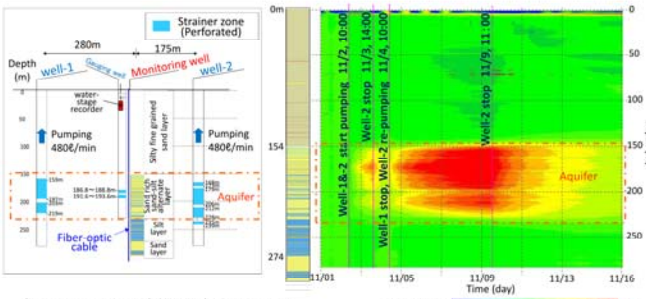


fig. 7 Compression of the aquifer by pumping

Strain -40με 40με

## 5. Distributed acoustic sensing (DAS)

- DAS allows seismic monitoring with fiber-optic cable and has developed recent years.
- A DAS applicability test was performed using the optic fibers which were already deployed behind the casing for the formation deformations monitoring.
- Through the stacked waveform obtained by the fiber included some noises, P-wave first break was able to be read as well as a geophone data.

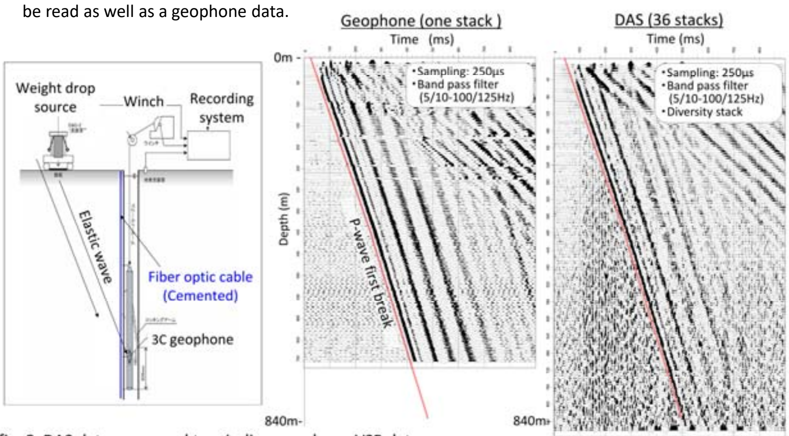


fig. 8 DAS data compared to wireline geophone VSP data

## 6. Future works

- Development and improvement of the high sensitivity and high strength fiber optic cable with the installation behind the casing.
- Improvements of the temperature, pressure and strain separation technique with the hybrid Brillouin-Rayleigh processing.
- Automation of data processing and analysis, realization of remote operation, and packaging of the observation equipment.

*This work is part of an R&D project "the Development of Safety Management Technology for Large-Scale $CO_2$ Geological Storage, commissioned to the Geological Carbon Dioxide Storage Technology Research Association by the Ministry of Economy, Trade and Industry (METI) of Japan.*

RITE
Research Institute of Innovative Technology for the Earth